Low frequency Raman spectroscopy of supercooled fragile liquids analyzed with schematic mode coupling models

C. AlbaSimionesco and M. Krauzman

Citation: The Journal of Chemical Physics **102**, 6574 (1995); doi: 10.1063/1.469373
View online: http://dx.doi.org/10.1063/1.469373
View Table of Contents: http://scitation.aip.org/content/aip/journal/jcp/102/16?ver=pdfcov
Published by the AIP Publishing

Low frequency Raman spectroscopy of supercooled fragile liquids analyzed with schematic mode coupling models

C. Alba-Simionesco
C.P.M.A., Batiment 490, Université de Paris-Sud, 91405 Orsay Cedex, France

M. Krauzman
D.R.P., Tour 22, Université Paris VI, 75252 Paris Cedex 05, France

(Received 21 March 1994; accepted 13 January 1995)

Recent experimental studies of the glass transition of molecular liquids have exploited light scattering techniques in order to support the dynamical model proposed by the mode coupling theory. In the framework of the dipole-induced-dipole (DID) formalism and the Stephen's approximation, we have checked this theory with several memory functions in the microscopic region, where phononlike excitations dominate, i.e., in the frequency window of 5–130 cm^{-1} accessible by a classical Raman spectrometer. The fitting procedure compares the experimental susceptibility spectra of one of the simplest fragile molecular liquid, *m*-toluidine, to the theoretical ones and estimates, in each case, the T dependence of the different control parameters as well as the crossing point of the transition line of type B. The agreement observed for spectra from a temperatures above the melting point down to the glass transition temperature T_g suggests, on the one hand, that information about the dynamical behavior of the supercooled liquid are contained in this frequency region and, on the other hand, that vibrational contributions are incorporated in this formalism, independently of the form of the relaxation kernel. Finally, the two-peak shape in the microscopic range of the susceptibility spectra is related to the relaxation of a linear combination of the Fourier components of the two density correlators. © *1995 American Institute of Physics.*

I. INTRODUCTION

Over the last decade the universal behavior of a wide variety of glass forming liquids has stimulated a great interest from the experimental as well as from the theoretical point of view. Whereas, the static properties of a supercooled liquid vary monotonously with the temperature down to a discontinuous change of the thermodynamic coefficients (the signature of the so-called calorimetric glass transition temperature T_g), the dynamic properties such as viscosity exhibit a strong temperature dependence. In particular, for ''fragile'' glass forming liquids, according to the Angell classification,[1] the viscosity shows a pronounced departure from an Arrhenius behavior and increases by several orders of magnitude over a short temperature range (30–50 K), near T_g at which finally, structural relaxations and molecular diffusions are stopped. This point is defined as an out of equilibrium amorphous solid; the glass. In an Arrhenius plot of the shear viscosity, two dynamical regimes are distinguished overcrossing around a certain temperature T_c: A power law at high temperature and a Vogel–Tamman–Fulcher temperature dependence at lower temperatures; this distinction has already been the object of careful attention. Assuming that the sudden increase of viscosity is governed by density fluctuations, the mode coupling theory[2] (MCT), the only available theory at the present time, proposes a bifurcation scenario for the liquid-glass transition and describes it as a purely kinetic transition from an ergodic liquid state to a nonergodic ideal glassy state; the singularity is expected to occur when the control parameters have a critical value which defines a critical temperature T_c well above T_g. On the other hand, around T_c and below, the contribution of activated hopping processes[3] increases and the decoupling of several relaxation processes has been observed.[4]

In order to extend the measurements over an extra temperature range into the supercooled liquid state, the first experimental act is to avoid the crystallization. Achieving this step is best understood by introducing the notion of a sort of chemical complexity. The ability to prevent crystallization is considered as a consequence of a poor packing efficiency of certain substances in the crystalline state in which the requirement of a three-dimensional order sets constraints on the molecular arrangements. It has been shown in earlier publications that the aromatic molecules (beginning with the simple toluene) are consistently more fragile than their saturated analogous and also that the lowest melting temperature members of a family of isomers can vitrify in an easier way.[5] Moreover, in a given family of molecules of the same shape, viz., a disubstituted benzene ring, an increase of the intermolecular strength from purely van der Waals to a stronger hydrogen bond or to dipolar interaction do not influence their fragile character.[6] In addition, for high coordination number ionic systems, recognized as constituting the second family of fragile glass forming liquids, their binary nature shows no influence on the dynamics near the glass transition as it appears from a comparison by computer simulation[7] of the MCT predictions on simple atomic liquid. Nevertheless, in spite of structural differences which produce particular properties, the control of the crystallization is not associated with the fragility: there exists fragile liquids which never crystallize and stronglike liquids which never vitrify (e.g., $AlPO_4$).

Recent light scattering experiments on ionic[8] or

 0021-9606/95/102(16)/6574/12/$6.00

molecular[9] liquids have shown that the dipole-induced-dipole (DID) light scattering mechanism appears as the most appropriate in the metastable supercooled state from above the melting point T_m down to the calorimetric glass transition (GT) temperature T_g and all experiments can be analyzed within the same theoretical background. In the frequency range of the Raman spectroscopy, typically from 5 to 130 cm^{-1}, our careful study of the depolarization ratio ρ supports the DID mechanism and the Stephen factorization will be used in our analysis.

The present work deals with several purposes. A first objective is to get general trends in the light scattering spectra of supercooled ''fragile'' liquids. The DID mechanism will appear as dominant in the vicinity of the glass transition whatever the complexity of the system. As a result, the intensity is proportional to the Fourier transform of the square of the density autocorrelation function, $\phi_q(t)$, which is the central theoretical concept of the MCT and is connected with experiments through the dynamical structure factor $S(q,\omega)$ as measured by inelastic neutron or light scattering.[10]

Accordingly, we propose a numerical comparison of the experimental susceptibility spectra to predictions of schematic MCT models, i.e., MCT models in which the memory function $M_q(t)$ is explicitly expressed as detailed in Sec. II. The whole temperature range of supercooling is scanned, and the spectral range is restricted to the microscopic area, where phononlike excitations coexist with fast relaxing processes. While the theory is usually checked in a spectral window of the GHz range with the help of master equations, our second objective is to estimate the degree of compatibility of the MCT critical approach in the THz domain when the vibrational contributions are incorporated in the dynamics of the transition. To begin with, it is required to get the long time evolution and the typical form of $\phi_q(t)$, the solution of an equation of motions containing a kernel $M_q(t)$. In order to avoid any *ad hoc* input for the memory function, we have built several models and tested the adequacy of their critical approach for one of the simplest molecular liquid: *m*-toluidine. In addition, because of the particular shape of the spectra, we have included in our analysis an extra mode different from the one at $q=q_0$ which corresponds to the maximum of the static structure factor, and we have tested their influences on the relaxation processes. The usual check of the scaling laws predicted by the theory is out of our scope.

II. EXPERIMENT

We have chosen an archetypal liquid, the *m*-Toluidine, a disubstituted benzene ring with the $-CH_3$ and $-NH_2$ groups in the 1,3 positions; it is one of the simplest fragile liquids usable as a representative example for the study of the supercooled range extending from the melting temperature $T_m=241$ K to the calorimetric glass transition $T_g=186.9$ K. All the spectra are presented in Fig. 1. Due to its retarded crystallization, a large collection of data on its thermodynamic and structural characteristics is available.[6,11]

Purchased at 99% of purity from Merck, the liquid has been distilled under vacuum, sealed in an annealed cubic Pyrex cell, and introduced in an Oxford Instrument cryostat. Raman spectra were taken with a Coderg T800 triple spectrometer driven by an IBM AT3 computer through a homemade interface. Photon counting during 1 sec each 0.125 cm^{-1}, was performed. Possible shifts of the frequency origin were corrected as a result of the best fit of Stokes to anti-Stokes spectra weighted by their corresponding inverse Bose–Einstein factor. The spectrometer was able to fully reject the parasitic light at frequencies above 4.5 cm^{-1}. For the sake of security, the spectra presented in this paper start at 5 cm^{-1}, the spectral end at 130 cm^{-1} is selected for being far enough from the internal mode influences and for having an intensity well above the weak luminescence or any other spurious background. Spectra of diffused laser light were also recorded in order to measure the net resolution resulting from the finite slit width and a cubic spline smoothing of the data: a linewidth of 1.9 cm^{-1} has been evaluated.

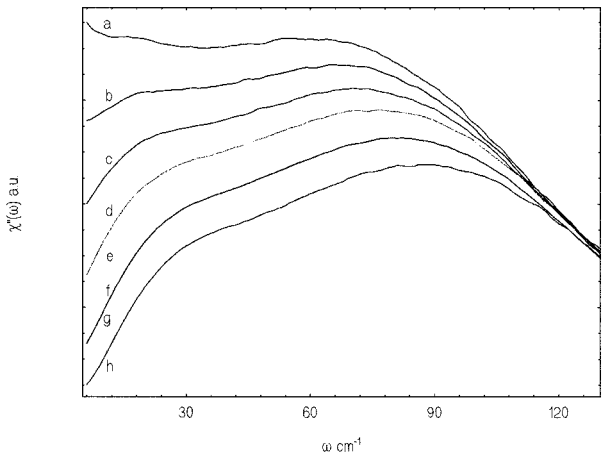

FIG. 1. Experimental susceptibility spectra $\chi''(\omega)$ at five temperatures above the calorimetric glass transition temperature $T_g=186.9$ K: (a) 290.5 K; (b) 264.3 K; (c) 239.1 K; (d) 214.9 K; (e) 193.5 K. Below T_g in the glassy state; (f) 189.3 K; (g) 175.4 K; (h) 127.9 K.

An Ar^+ laser providing a power of 200 mW at the 514.5 nm wavelength was used. All the spectra are presented in Fig. 1. The following cares were taken for the measurement of the depolarization ratio $\rho=I_{HV}/I_{VV}$ down to a temperature of 175 K.

(i) A systematic check of the quality of the laser beam propagation through the sample, the six cryostat windows, and the two cell walls. The loss of polarization was found to be less than 1%.

(ii) The polarization directions were adjusted by minimizing I_{HV} or maximizing the peak intensity of the ring breathing mode at 995 cm^{-1}, whose depolarization ratio ρ was found to be 5% and constant.

(iii) A slow alteration of the sample was observed, resulting in a slow increase of the incident and scattered light absorption. This effect was reduced by broadening the laser beam (i.e., focusing out of the sample cell). The remaining apparent efficiency loss has been measured and corrected by recording several times in alternate sequences the *VV* and *HV* polarized spectra.

The measurement of ρ has not been attempted below the aforementioned temperature of 175 K because the polarization of light is destroyed in the sample by the stress persistency in the highly viscous material. Our result is

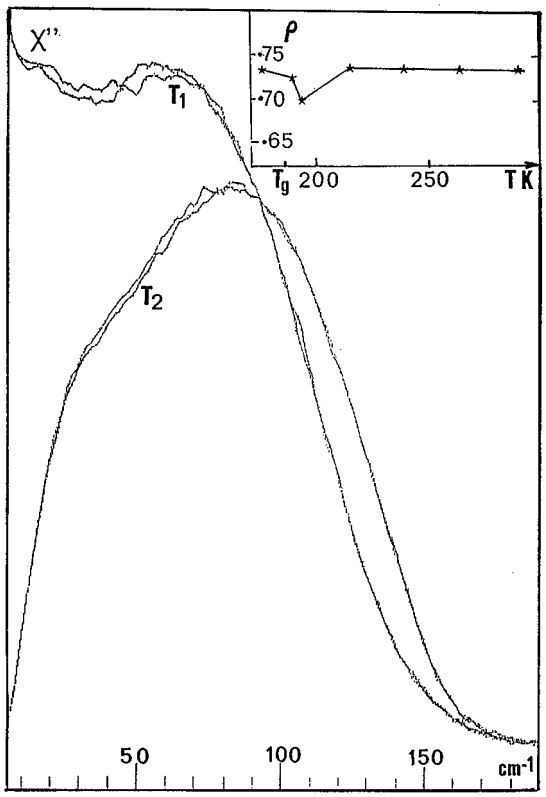

FIG. 2. Illustration of the frequency independence of the depolarization ratio ρ: $\chi''_{HV}(\omega)$ is compared to $0.73\chi''_{VV}(\omega)$ at T_1=290.5 K and T_2=175.4 K. Inset: T dependence of ρ.

$$\rho(\omega,T)=0.73\pm0.01.$$

Figure 2 illustrates the ω and T (insert) quasiindependence of ρ above 175 K.

III. SPECTRAL TRENDS AND DID MECHANISM

In the supercooled regime of the liquid, after a normalization of the experimental spectra by the inverse Bose–Einstein factor $[1/(\bar{n}(\omega)+1)]$, with $\bar{n}(\omega)=[\exp(\hbar\omega/kT)^{-1}]^{-1}$ in order to compare with the susceptibility spectra $\chi''_{\text{calc}}(\omega)$ computed from schematic MCT models [cf. Eqs. (3.3) and (3.4)]. The main finding is an anomalous excess of intensity in the low frequency part when temperature increases, while the rest of the shape remains almost unchanged. The use of a higher resolution tandem Fabry–Perot spectrometer at smaller frequencies has established that it is not produced by a broadening of the central quasielastic line. The extra intensity is due to relaxational processes found between the structural relaxation α and vibrational motions, which may be called ''fast'' β-processes in order to distinguish them from the usual (or ''slow'') β processes[12] encountered either above T_g by nuclear magnetic resonance (NMR) spin lattice relaxation or below T_g by dielectric relaxation measurements. The fast β process defined by inelastic light scattering (ILS) is related to correlation times from 10^{-10} to 10^{-12} sec, while the original β relaxation is slower, 10^{-4} to 10^{-6} sec, and difficult to identify at high temperature since it is often masked by the high frequency wing of the α-resonance. As suggested by Rössler[4], the ILS fast-β and the NMR slow-β processes can be regarded as the short- and the long-time tail of a single physical mechanism precursor of the slowing-down dynamics of glass forming liquids.

The same features were first revealed in several systems (ionic,[12] molecular,[13] and polymeric[14]) by neutron scattering like time-of-flight (TOF) experiments.[15] Moreover ILS and TOF both allow to distinguish between pseudo phonons and relaxation, the ratio of those two contributions having been recently related to the ''strength''[10] of several supercooled liquids; the overlap of the two contributions may contain the origin of an incompatibility of the MCT model with strong or intermediate liquids,[16] provided the analysis of the microscopic peak is properly done in such liquids.

Another current finding in the spectra is the double hump shape of the dynamical susceptibility $\chi''(\omega)$ in many aromatic fragile liquids, such as salol, *o*-terphenyl, *m*-toluidine, *m*-cresol, *m*-fluoroaniline[17] with the two maxima around 20 and 70 cm^{-1}. This structure is often hidden in a log–log plot of χ'' and associated to a so-called microscopic peak, which provides the upper frequency limit of the relaxation times. The existence of a second hump seems to impede the application of the extended version of MCT, only valid, thus far, for the ionic liquid K–Ca–NO_3(CKN).[18] The examination of this effect is not yet in our purpose and will be developed in further work.

The light scattering spectrum in an isotropic fluid is related to the polarizability fluctuations dominated by the DID process contribution, which involves a four body density correlation function. The Stephen's factorization[19,20] leads to a more tractable expression of a sum of products of two point correlation functions. The effect of such a factorization has already been discussed in detail in the literature for the shape of the spectra,[21] as well as for the predicted intensity of the spectra[22] since controversial considerations seem to emerge depending on authors. The spectral shape is commonly regarded as the convolution product of the dynamical structure factors:

$$I^{\text{Raman}}(\omega)\propto[1+\tfrac{1}{3}(\hat{\mathbf{E}}_S\cdot\hat{\mathbf{E}}_0)^2]\int\int d^3q\ d\Omega\ S(q,\Omega)S\times(-q,\omega-\Omega). \tag{3.1}$$

The main characterization of this mechanism is the depolarization ratio $\rho(\omega)$: in a 90° scattering experiment, the product $\hat{\mathbf{E}}_S\cdot\hat{\mathbf{E}}_0$ of the unit vectors of the incident and scattered electric field equals 1 and 0, respectively, in the *VV* and *HV* configurations. Thus $\rho(\omega)$ is theoretically equal to 0.75. In our measurement, in the case of *m*-toluidine, but also in all fragile glassformers studied thus far, $\rho(\omega)$ remains close to this theoretical value indicating that the dominant scattering mechanism is the DID in a very broad temperature range.

According to Tao *et al.*,[20] we may rewrite Eq. (3.1) in terms of the products of correlators with the definitions:

$$S(q,\omega)=S(q)\phi''(q,\omega), \tag{3.2}$$

$$\phi''(q,\omega)=\int_0^\infty \cos\ \omega t\,\phi_q(t)dt\equiv\text{Im}\{FT[\phi_q(t)]\}. \tag{3.3}$$

One then arrives at

$$I^{\mathrm{Raman}}(\omega) \propto \mathrm{Im}\left[FT\left(\int dq\ 4\pi q^2 S^2(q) \phi_q^2(t) \right) \right]. \quad (3.4)$$

A similar result has been obtained by Fuchs and Latz[23] who expressed, in the framework of MCT formalism, the intensity of the depolarized light scattering spectra reflecting the fluctuations of the dielectric constant coupled to density pair correlators.

A nonconvoluted $\phi''(q,\omega)$ was proposed by Cummins *et al.* for the comparison of the experiments with MCT predictions and the application of the master equations at $T \geqslant T_c$ in the vicinity of the minimum of the susceptibility spectra $\chi''(\omega)$: The effective susceptibility extracted from ILS data is stated as indistinguishable from the susceptibility of TOF data, except in the α-peak region. On the other hand, Watson and Madden[24] have pointed out in a recent computer simulation study that the DID spectrum refers mainly to a quadratic term in the density correlators. Here no assumptions are needed at any temperatures for the quantitative prediction of the temperature evolution of the Raman spectra approaching the glass transition; consequently, in the following, the convolution of $\phi''(q,\omega)$ is systematically and easily calculated.

The greatest weight of the integral of Eq. (3.4) is supplied by modes with q near the principal peak at q_0 of the structure factor $S(q)$; nevertheless, in molecular liquids the spectra might be influenced by density fluctuations with smaller wave vectors. In order to properly represent the experimental spectral shapes described earlier, we postulate that another q is involved in the integral. The associated density correlator contributes to the scattered intensity in the microscopic time domain as

$$I^{\mathrm{RAMAN}}(\omega) = A_{q_0}^*\ \mathrm{Im}\{FT[\phi_{q_0}^2(t)]\} + A_{q_1}^*\ \mathrm{Im}\{FT[\phi_{q_1}^2(t)]\}$$
$$= B^*\ \mathrm{Im}\{FT[\phi_{q_0}^2(t) + \gamma^* \phi_{q_1}^2(t)]\}, \quad (3.5)$$

where γ is the relative weight of this second contribution. B^* is allowed to vary with temperature in order to include eventual ''cancellation effects'' of the DID scattering.

As revealed by computer simulation studies,[24] the q dependence of the light scattering spectra in the vicinity of the glass transition may be significant. q effects contribute to the spectra in two respects: first it produces an excess scattering in the very low frequency domain and shifts the α resonance; secondly, an additional peak to the main microscopic peak appears in the same way as the double hump shape of the experimental spectra. This is in agreement with a second correlator at a different q introduced earlier. Furthermore, other fluctuations may be taken into account in the DID mechanism such as the concentrations, the charges, or the stress fluctuations.

IV. THE MCT FORMALISM

The mode coupling theory[2] provides qualitative explanations of the dynamics of a supercooled liquid and predicts scaling properties in the GHz domain, including the characteristic stretching effects of the structural relaxation near the glass transition. The density fluctuations are slowing down when approaching a critical point and the overdamped response $\phi_q(t)$ is the solution obeying $\phi_q(0)=1$ of a generalized Langevin equation of motions expressed in the time space:

$$\ddot{\phi}_q(t) + \Omega_q^2 \phi_q(t) + \Gamma_q \dot{\phi}_q(t) + \Omega_q^2 \int_0^t M_q(t-t') \dot{\phi}_q(t')\, dt' = 0, \quad (4.1)$$

where q is a wave vector, Ω_q is the characteristic microscopic frequency of the liquid, Γ_q is a damping constant, and the overdots denote time derivatives. In other words, the low frequency behavior of the spectra susceptibility can be calculated via the density spectrum $\phi''(q,\omega)$ defined in Eqs. (3.2) and (3.3). The memory function $M_q(t)$ describes the interactions between density fluctuations modes:

$$M_q(t) = F_q[V, \phi_k(t)] \equiv \Sigma_{kp} V(q,k,p)\, \phi_k(t)\, \phi_p(t), \quad (4.2)$$

where the control parameters $V(q,k,p) \geqslant 0$ can be expressed in terms of microscopic parameters of the system; they depend smoothly on density and temperature. Thereby, the cage effect treatment of cooperative motions in dense liquids is valid until certain critical values of the temperature and the density, which involve the existence of an ideal liquid-glass transition.

In the liquid state, the correlator decays to zero at long times. In the ideal glassy state, where the tagged particle motion becomes nonergodic, the correlator is arrested at some positive value $f_q = \lim_{t\to\infty} \phi_q(t)$; f_q is called the Debye–Waller factor of the frozen liquid (also the nonergodic parameter, Edwards–Anderson parameter, etc.) and is the largest solution of the infinite time limit of Eq. (4.1):

$$f_q/(1-f_q) = F_q(\vec{V}, f_q). \quad (4.3)$$

The transition surface between the two states in the control parameter space is made of bifurcation singularities; therefore an index c (for critical) is added to the notation of the vertices $V_c(q,k,p)$, the order parameter f_{qc} and the temperature T_c on this surface. While all equilibrium thermodynamic functions behave regularly across this surface, the characterization of this transition is associated with a discontinuity in f_{qc} as in the type B transition[25] and correlation functions can be discussed in terms of scaling laws.

The vertices govern an exponent parameter λ which determines the scaling law exponents of the relaxation processes near the critical temperature around the susceptibility minimum: a for the high frequency side and b for the α-relaxation side, in the following equation of Γ functions:

$$\lambda = \Gamma^2(1-a)/\Gamma(1-2a) = \Gamma^2(1+b)/\Gamma(1+2b). \quad (4.4a)$$

The generic time behavior of the density fluctuations $\phi_q(t)$ for a given wave vector q begins at very short times on the order of the inverse microscopic frequency $t_0 = 1/\Omega_q$, and outside the transient region it is described by a first power law decay,

$$\phi_q(t) = f_{q_c} + h_q (t/t_0)^{-a}, \quad (4.4b)$$

and reaches a second power law regime called the von Schweidler regime, where

$$\phi_q(t) = f_{q_c} - B h_q (t/\tau_\alpha)^{-b}. \quad (4.4c)$$

The exponent b is related, in one case labeled as the F12 model, to the β exponent of the stretched exponential of the Kohlrausch–Williams–Watt law for the α relaxation:

$$\phi_{KWW}(t) \propto \exp -(t/\tau_\alpha)^\beta. \tag{4.4d}$$

The exponents are not universal as for conventional critical phenomena; furthermore, within their validity range, they take values which depends on the kernel in Eq. (4.2).

One strong usual assumption of the MCT is that the relaxation processes are supposed to be dominated by the modes at $q=q_0$ (corresponding to the inverse molecular nearest-neighbor distance) where the first peak of the static structure factor occurs.[26]

In its original version, the MCT describes the dynamics of the α relaxation only above T_c. For experiments on α peak below T_c, an extended version including activated hopping processes is available. This extension does not influence neither the microscopic range nor the fast β processes; in a further computation,[18] it clearly appears that at least for the molecular liquid studied so far, i.e., the salol, the presence of a second hump below the microscopic peak prevents from extending the theory to the high frequency side of the susceptibility minimum for $T<T_c$.

Since a double hump exists in the shape of the susceptibility spectra of many fragile liquids, it seems natural to incorporate in the model a second correlator at a different wave vector q_1 with specific Ω_{q_1} and Γ_{q_1}. A similar kernel $M_{q_1}(t)$ enters the second dynamic equation:

$$\ddot{\phi}_{q_1}(t)+\Omega_{q_1}^2\phi_{q_1}(t)+\Gamma_{q_1}\dot{\phi}_{q_1}(t) + \Omega_{q_1}^2\int_0^t M_{q_1}(t-t')\dot{\phi}_{q_1}(t')dt'=0 \tag{4.5}$$

with a third control parameter r,

$$M_{q_1}(t)=rM_{q_0}(t). \tag{4.6}$$

The addition of a second correlator has already been introduced by Sjögren[27a] and by Bosse and Krieger[27b] in a more general model of density and charge fluctuations. Generalizing this notion, we apply several relaxation kernels, containing some nongeneric peculiarities that are presented later. In each case, a type B transition line or surface defines the critical values of the control parameters and of the order parameter. In all cases, at the transition, the two order parameters jump simultaneously to a nonzero value.

A primary model, called the F2 model, contains the kernel $M_{q_0}(t) = v_2\phi_{q_0}^2(t)$ and produces an α resonance below a microscopic peak, but no stretching is obtained. Therefore the model does not agree with the description of the glass transition. As noticed by Götze,[2] all kernels proportional to ϕ^n with $n\geqslant 2$ yield the same properties. We will return to this point later in the discussion of one of our two correlator models.

The stretching in the α relaxation is introduced with the addition of a linear term in M_q generating the following F12 model now with two correlators:

$$\text{F12:}\quad M_{q_0}(t)=v_1\phi_{q_0}(t)+v_2\phi_{q_0}^2(t),$$

$$M_{q_1}(t)=rM_{q_0}(t). \tag{4.7a}$$

The transition is defined by

$$v_{1c}=-v_{2c}+2(v_{2c})^{1/2} \tag{4.7b}$$

and the Debye–Waller factors are

$$f_{0c}=1-1/(v_{2c})^{1/2}$$

and

$$f_{1c}=r[(v_{2c})^{1/2}-1]/\{1+r[(v_{2c})^{1/2}-1]\} \tag{4.7c}$$

and the exponent parameter is

$$\lambda=v_{2c}^{-1/2}. \tag{4.7d}$$

Another model, called the F13 model, introduces a correlator to a higher power:

$$\text{F13:}\quad M_{q_0}(t)=v_1\phi_{q_0}(t)+v_3\phi_{q_0}^3(t),$$

$$M_{q_1}(t)=rM_{q_0}(t). \tag{4.8a}$$

The critical quantities are solutions of the following set of equations:

$$v_{1c}=(1-3f_{0c}/2)/(1-f_{0c})^2,\quad v_{3c}=[2\ f_{0c}(1-f_{0c})^2]^{-1},$$
$$x=rf_{0c}(v_{1c}+v_{3c}f_{0c}^2),\quad f_{1c}=x/(1+x), \tag{4.8b}$$

and the exponent parameter is given by

$$\lambda=3(1-f_{0c})/2. \tag{4.8c}$$

In the preceding models, the equations are not symmetrical with respect to the interchange of the correlators. We have developed a symmetrical model, called the F0F1 model:

$$\text{F0F1:}\quad M_{q_0}(t)=c_0\phi_{q_0}(t)\phi_{q_1}(t),$$

$$M_{q_1}(t)=c_1\phi_{q_0}(t)\phi_{q_1}(t). \tag{4.9a}$$

The transition line is conveniently expressed in term of d_i, the parameters inverse roots $d_i=1/(c_i)^{1/2}$;

$$d_{0c}+d_{1c}=1, \tag{4.9b}$$

$$f_{0c}=d_{1c}\quad\text{and}\quad f_{1c}=d_{0c}. \tag{4.9c}$$

A nongeneric property of this model results from the constant value $\lambda=0.5$ all along the transition line:[28] as in the F2 model, there is no stretching, even in the bidimensional $\vec{V}$ space of the present model.

This defect is eliminated in our fourth model, where a linear term is introduced in the kernels, which removes the symmetry of the equations. This model is called F0F01;

$$\text{F0F01:}\quad M_{q_0}(t)=v_{01}\phi_{q_0}(t)\phi_{q_1}(t)+v_0\phi_{q_0}(t),$$

$$M_{q_1}(t)=rM_{q_0}(t). \tag{4.10a}$$

On the transition surface, defined by

$$v_{01c}=[(1-v_{0c})^{1/2}+1/(r_c)^{1/2}]^2, \tag{4.10b}$$

the critical values of the order parameters are

$$f_{1c}=(v_{01c}-v_{0c}+1-1/r_c)/(2v_{01c}), \tag{4.10c}$$

TABLE I. Listed fixed parameters.

Models	Ω_{q0} (cm^{-1})	Γ_{q0}	Ω_{q1} (cm^{-1})	Γ_{q1}	γ	r	D (%)
F12	38.3	1.14	9.86	3.14	0.585	2.60	1.0
F13	34.8	1.30	8.94	2.70	0.375	2.35	0.9
F0F1	40.9	1.34	15.3	3.93	1.013		1.0
F0F01	39.0	1.32	24.7	3.56	0.812	0.682	1.1

$$f_{0c}=[r_c(v_{01c}+v_{0c}-1)+1-2v_{0c}]/[2(r_c v_{01c}+r_c v_{0c}-v_{0c})]. \quad (4.10d)$$

The corresponding exponent parameter λ has not been calculated. The phase diagrams of these models are represented in Fig. 4 and explained later in the context of the experiments.

It is always possible to create new models incorporating nongeneric features responsible for particular properties of a given system, by changing the combination of the correlators, adding other correlators, referring to other fluctuations or correlators of higher degrees, giving rise to more complex phase diagrams. In return, the number of fitting parameters is increased and, therefore, reduces the physical significance of the probed models.

V. DATA PROCESSING

In order to check the agreement of the MCT equations (4.1) and (4.5) with our experimental results, we have proceeded as follows.

(i) A step by step numerical resolution of the equations of motion of the two correlators was based on the following recurrent relations:

$$\phi_i^{n+1}=\phi_i^n+\dot{\phi}_i^n dt+\ddot{\phi}_i^n dt^2/2, \quad (5.1)$$

$$\dot{\phi}_i^n=(\phi_i^{n+1}-\phi_i^{n-1})/2dt, \quad (5.2)$$

where dt is the time step of the calculation, $\phi_i^n=\phi_i(ndt)$ and $\ddot{\phi}_i^n$, is extracted from the equations in the preceding section according to the selected model. The initial conditions are $\phi_i^0=1$ and $\dot{\phi}_i^0=0$.

(ii) As discussed previously, the link between the theoretical calculation and experiments is conventionally achieved by comparing the experimental susceptibility

$$\chi''_{\rm exp}(\omega)=I^{\rm Raman}(\omega)/[(n(\omega)+1)] \quad (5.3)$$

to the susceptibility calculated in agreement with the DID theory,

$$\chi''_{\rm calc}(\omega)\propto\omega\ {\rm Im}\ FT[\phi_{q_0}^2(t)+\gamma\phi_{q_1}^2(t)], \quad (5.4)$$

where Im FT is a fast cosine Fourier transform.

The following values of constants were selected for a compromise between a sufficient precision and a reasonable duration of the calculations: number of steps $N=512$, frequency step $d\omega=1\ cm^{-1}$ and time step $dt=1/(2Nd\omega)$.

(iii) All these calculations were part of a classical least square fitting procedure, performed on a desk personal computer. It was applied simultaneously to five spectra averaging multiple scans at the five experimental temperatures listed in Fig. 1.

The frequencies Ω_{q0}, Ω_{q1}, and the widths Γ_{q0}, Γ_{q1}, of the oscillators, the control parameter r, in Eqs. (4.1), (4.5), and (4.8), and the coefficient γ of Eq. (4.6) were taken as temperature independent, while a scale factor and the two control parameters were allowed to vary freely with the temperature T; all fixed parameters are listed in Table I. For each model, the path of the control parameters crossing the transition line is plotted on Fig. 5(a). Their T dependence is represented in Fig. 5(b) and their critical values are given in Table II.

VI. RESULTS AND DISCUSSION

Until now the mode coupling theory is the only available theory adequately predicting the structural relaxation dynamics and the shape of the susceptibility spectra around the minimum observed in light scattering and neutron scattering experiments in the supercooled liquid. In the present work, we have compared the predictions of the MCT equation to our experimental data in the range of 5–130 cm^{-1}. Fortunately, the high statistical accuracy of the Raman scattering data allows us to distinguish between several models of memory functions and to give a quantitative estimation of their parameters, provided they are not too numerous.

As a result of the data processing described above, we present in Fig. 3 (in a linear and in a logarithmic scale in ω) the experimental susceptibility spectra compared to the cal-

TABLE II. Critical values of the control parameters crossing the transition line.

		Parameters at T_c				
Models	T_c (K)			λ	f_{0c}	f_{1c}
F12	235.2	$v_{1c}=0.043$	$v_{2c}=3.91$	0.505	0.495	0.718
F13	234.3	$v_{1c}=0.944$	$v_{3c}=4.21$	0.713	0.524	0.722
F0F1	253.3	$c_{0c}=3.27$	$c_{1c}=5.01$	0.500	0.447	0.553
F0F01	249.8	$v_{0c}=0.640$	$v_{01c}=3.28$	>0.5	0.421	0.331

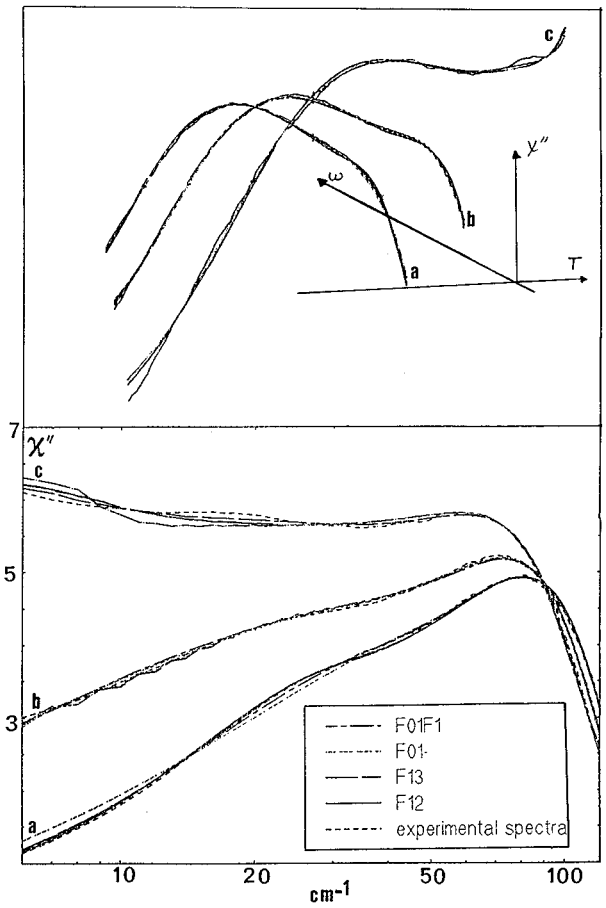

FIG. 3. (1) Linear ω-scale and (2) logarithmic ω-scale plots of experimental (squares) compared to calculated $\chi''(\omega)$ at (a) 193.5 K, (b) 239.1 K, and (c) 290.5 K, for the four models. The equally good qualities of the adjustments prevent from distinguishing between the models F12 (dotted curve), F13 (solid curve), F0F1 (dotted-dashed curve), F0F01 (dashed curve) as explained in the text.

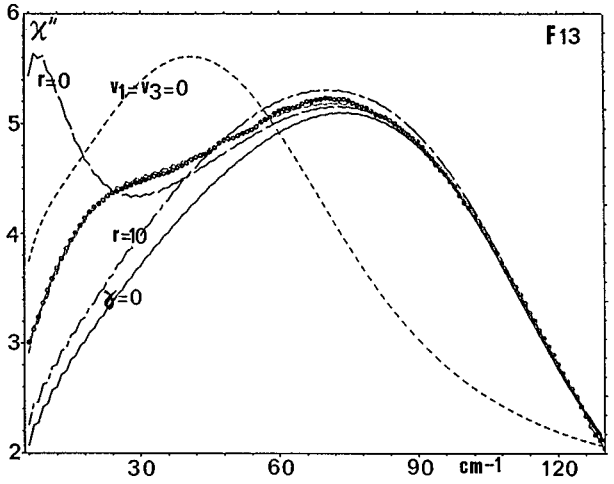

FIG. 4. Influences of the parameters: the experimental spectrum (●) at $T=239.1$ K is superimposed to the fitted F13-model (solid line). The other curves illustrate the effect of modifying various parameters: $r=0$, dotted-dashed line; $r=10$, dashed line; $\gamma=0$, solid line; $v_1=v_3=0$, dotted line.

culated spectra resulting from the two correlator models F12, F13, F0F1, and F0F01 at three characteristic temperatures: in the liquid at $T=290.5$ K, in the supercooled regime at $T=239.1$ K ($T_g/T=0.78$), and slightly above T_g at $T=193.5$ K. The corresponding relative root mean square deviations D are given in the last column of the Table I. Regarding the high quality of the fits reflected by D, it is difficult to select one model and it strongly supports the formalism applied at least over 1.5 decades in frequency.[29] A relative classification of the kernels would be possible with a broader frequency range of data, covering namely the vicinity of the minimum of the susceptibility spectrum. Because we have tested the MCT in the THz regime, it was important to provide a precise determination of the microscopic band of the model, which is usually not taken into account. Table I shows that the characteristics of the microscopic modes of the studied liquid are only slightly dependent on the models. The frequency of the main correlator lies between 35 and 41 cm^{-1} and the frequency of the second one slightly depends on its adherence to the kernel, as well as its contribution, defined by γ, to the total susceptibility and the coupling parameter r, while all damping coefficients Γ_{qi} remain constant. Two elements govern the short time transient motion of each correlator: the frequency Ω_q and its damping coefficient Γ_q. The microscopic time scale defined by $t_0=1/\Omega_{q0}$ and $t_1=1/\Omega_{q1}$ does not affect the master functions. The transient microscopic motion produces the first 20% of the total decay for temperatures close to T_c, and continues by other decay laws (see Fig. 7). In all models, the main correlator ϕ_{q0} controls the dynamics of the system and the contribution of the additional one to the scattered intensity is smaller ($\gamma<1$), except for the symmetrical model F0F1 where the two contributions are equivalent. In Fig. 4, a spectrum calculated with the F13 model at $T=239.1$ K is plotted without the second correlator (case $\gamma=0$); it shows how the form of the low frequency part of the susceptibility is modified by the latter contribution. This point illustrates the difficulty of estimating the exponent of the fast β process in aromatic supercooled liquids; moreover, it proposes a way to remove the uncertainties originated in the microscopic aspects of a given system. The treatment of the data in the THz domain requires the knowledge of the dynamics of the system and a specified memory function. Figure 4 illustrates the effect of the memory function on the frequencies of the maxima: the phonons cannot be disconnected from the relaxational part and a strong difference exists between the bump frequencies, the Ω's values, and the simple anharmonic oscillator maximums (i.e., $v_i=0$); their straightforward quantitative measurements in the spectra remain doubtful.

The analysis of the fast relaxation processes in TOF experiments[14b] has enlightened the complexity of the problem: a deconvolution procedure in the time domain of the experimental intermediate scattering function $I(q,t)$ and the overlapping time scale between the phononlike and the β_{fast} process contain strong uncertainties and often lead to incorrect values of the exponent parameter a (and λ). The data treatment proposed here is more direct and presents the advantage to include the microscopic excitations in the calculation which avoids the speculations on the phononic contribution.

Finally, in addition to the vertices of the kernel, the third

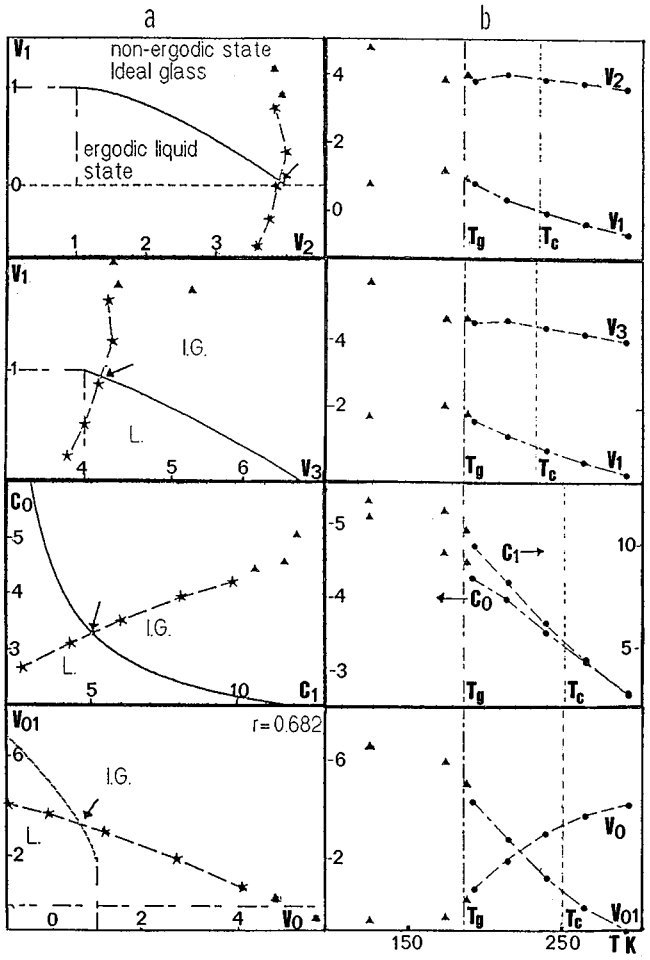

FIG. 5. (a) Phase diagram for the (1) F12, (2) F13, (3) F01, and (4) F0F01 models. The solid lines are the transition lines from an ergodic to a nonergodic state. The control parameters (⋆) fitted to the experimental data are connected with a dashed eye guide line. The values for $T<T_g$ plotted with full triangles have not been taken in the fitting procedure. The arrow points towards the critical singularity. (b) T dependence of the control parameters for the same models.

control parameter r has been taken as T independent; it does not influence the occurrence of the critical singularity, except in the last F0F01 model. Figure 4 illustrates how this parameter modifies the spectrum in two cases: $r=0$ and $r=10$, the latter resulting in a stretching and a flattening of the second correlator.

The distinction between the models comes out of their dynamical characterization, viz., the control parameters, which are the other important output of the fitting procedure. Usually the vicinity of the transition is implicitly described by a linear temperature dependence of a control parameter. For the first time, the path from one regime (liquid) to the other (ideal glass) in the V-phase diagram, the transition point and the temperature dependence of the control parameters are shown in Figs. 5(a) and 5(b). When a control parameters happens to take a negative value, then it sets an upper temperature limit of the corresponding case. The characterization of the dynamical singularity depending on the models is summarized in Table II. The critical temperatures are calculated by interpolating the fitted control parameters at the experimental temperatures across the transition line and are to be taken solely as indicative values; however, the critical temperatures obtained in this way from the first two models are in agreement with the ratio usually found for fragile glass forming liquids ($T_g/T_c=0.8$). The present work, where only two decades are scanned, does not allow a detailed analysis or test of the master functions provided by the MCT; however, the quantitative evaluations of the parameters given in Tables I and II is useful for the understanding of the effects of the control parameters in a light scattering experiment. In the first two models, the T dependence of the DID spectrum is mainly driven by the coefficient of the linear term in ϕ_{q0}, while the quadratic or higher term coefficients are not very depending on T.[29] In the two other models, all parameters play an equally important role in the temperature behavior of the spectrum. In all models, the control parameter T variation is smooth from the liquid state, across the singularity at T_c, down to T_g where one notices a change in their slopes in relation with the disappearance of the extra intensity below T_g.

From the critical value of the control parameters at the transition, other critical parameters are deduced: the exponent parameter λ, which is crucial for the calculations of the scaling laws of the correlation functions, and the associated order parameter jump (from 0 to f_c). The results are given in Table II for each correlator of every model. The exponent parameter λ requires some comments. It dominates the characterization of all the relaxation processes around the dynamical singularity that is around the curvature maximum of the viscosity in an Arrhenius plot. λ can also be related to the stretched exponent β of the Kohlrausch–Williams–Watt relaxation function well adapted to the analysis of the structural relaxation: the smaller λ is (=0.5), the higher β is (=1). The influence of this parameter is shown in Fig. 6, where the calculations with every model of the susceptibility spectra are extrapolated to a lower spectral range at two different temperatures: 264.3 K, which is systematically in the ergodic phase, and 239.1 K, which is closer to T_c and in some cases in the nonergodic phase (without an α peak). The α peak is apparently broader (i.e., smaller β) for models with larger λ. The value of λ=0.713 given by the F13 model seems more realistic when compared to other data of the literature: salol; λ=0.70 from ILS, CKN; λ=0.81 from ILS, *o*-terphenyl; λ=0.70 from ILS, and λ=0.77 from TOF experiments. However, the lack of a complete comprehension of the light scattering mechanism puts some doubts on its definitive value.

Outside the transient relaxation ($\omega<\Omega_0$ or $t>t_0$) the scaling laws of the relaxational processes are usually described by a master function in the GHz range for temperatures very close to the temperature T_c. Our approach is quite different by the direct use of the correlator time functions. As activated processes are neglected, the curves decay to a plateau value f_{qc} corresponding to the divergence of the shear relaxation time. Therefore, the analysis presented here is expected to have a physical relevance only above T_c. However the α resonance occurs at a frequency well below the frequency window studied in this paper, leaving our analysis still valid: a single explanation is applied from the stable equilibrium liquid ($T>T_m$) down to the nonequilibrium

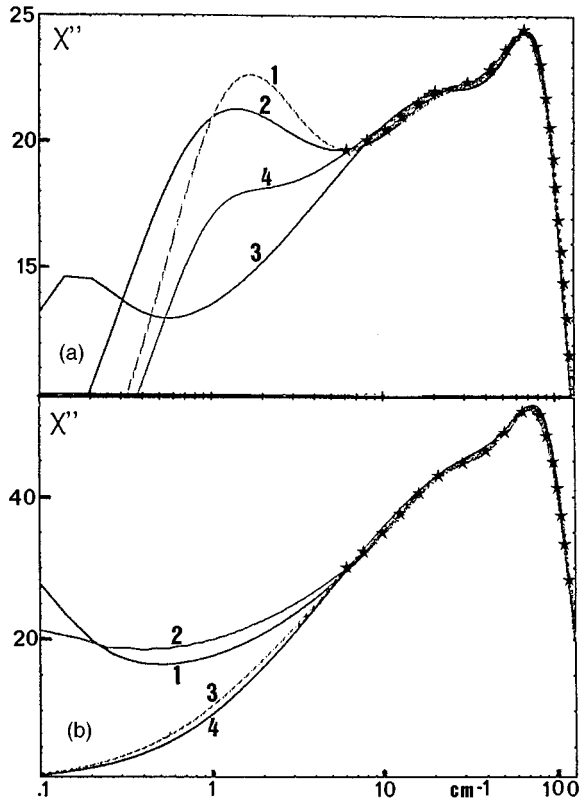

FIG. 6. Experimental data (⋆) at (a) 264.3 K and (b) 239.1 K and the fitted susceptibility spectra extrapolated to low frequencies. For the 4 models: (1) F12; (2) F13; (3) F0F1; (4) F0F01.

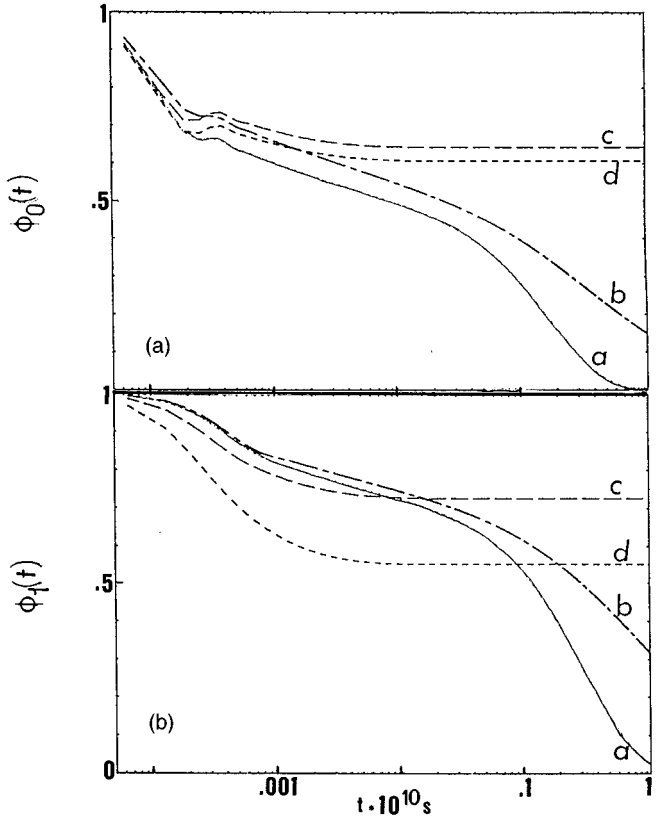

FIG. 7. Extrapolation of the density correlators to long times (1) $\phi_{q0}(t)$ and (2) $\phi_{q1}(t)$ at $T=239.1$ K of (a) the F12 [for which $\epsilon=(T-T_c)/T_c=0.017$], (b) the F13 ($\epsilon=0.020$), (c) the F0F1 ($\epsilon=-0.056$), and (d) the F0F01 ($\epsilon=-0.043$) models. These correlators were steps in the calculations of $\chi''(\omega)$ of Fig 6(b).

glass ($T<T_g$) without any temperature cutoff. The two correlators ϕ_{q1} and ϕ_{q0} given by the numerical resolutions of Eqs. (4.1) and (4.3) are plotted in Fig. 7 for $T=239.1$ K and extrapolated up to longer time. At this temperature, the long time decays of the correlators are vanishing for the F12 and F13 models (as $T>T_c$), but are finite for the F0F1 and F0F01 models ($T<T_c$).

The second peak in the calculated spectra results from the addition of a second correlator at a wave vector q_1, distinct from q_0, with a frequency $\Omega_{q1}<\Omega_{q0}$. It may be assigned to propagating shear modes. These modes have been observed in the liquids studied so far, even in the region of very low viscosity, provided that the shear mode frequency is larger than the α-relaxation time. On the other hand, the frequency of the bump of lower energy is strongly temperature dependent. In the present work we have assumed that the bare oscillators frequencies as well as their damping coefficients are T independent, the extraintensity on the low frequency side being caused by memory effects. The existence of a second active wave vector was already pointed out in the case of CKN by Mezei *et al.*[13] by analogy to the so-called de Gennes narrowing. The observed q dependence of the characteristic relaxation time τ_α presents at all temperatures an unexpected peak near $q_1=0.8$ Å^{-1} not discernible in the neutron static structure factor $S(q)$ and distinct from the main peak in $S(q)$ at $q_0=1.9$ Å^{-1}; this extra wave vector corresponds to a cation–cation (or anion–anion) distance and induces a dynamical correlation for ionic systems; moreover, we note that a low frequency bump is observed in the susceptibility spectra below T_g. In the same way, in aromatic liquids (like *m*-toluidine, *o*-terphenyl, salol, etc.) electric forces can stabilize a configuration of the molecules which promotes a similar q dependence of the structural relaxation time; this is supported by the observation, in all supercooled aromatic liquids,[11,30] of a splitting of the mean structural peak into two maxima which behave differently with temperature; however, this point needs to be completed by extended studies of $S(q)$ at $q<q_0$ in the supercooled liquid and the corresponding crystal, which are in progress.[11]

All along the preceding discussion, we have affirmed that the dominant correlator, at q_0 is related to the main peak of $S(q)$, and that the other correlator contributes only partially to the dynamics of the system [see Fig. 8(a)]. In order to check this statement, the models were fitted again with the lower frequency bound to q_0 in contrast with the preceding results where the free fitted frequencies were obtained in the proper order. Results are given in Table III and Fig. 8(b) illustrates the case of the F13 model at $T=264.3$ K. In the insert is presented the unrealistic result that the values of the control parameters plotted in the phase diagram are all contained in the ideal glassy state domain and consequently there is neither a transition nor any α peak in the susceptibility spectra even at high temperature. One is led to the conclusion that the previous hierarchy of the correlators has

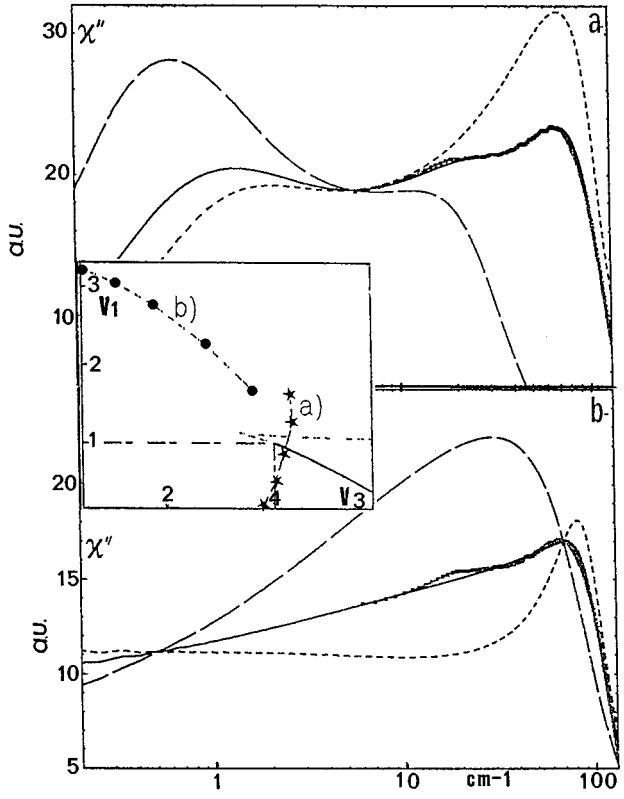

FIG. 8. Partial contributions $\chi''_{q0}(\omega)$ (dotted line) and $\chi''_{q1}(\omega)$ (dashed line) to the total susceptibility spectra (solid line) of the F13 model fitted to the experimental spectrum at $T=264.3$ K ($\star$). (a) Normal fit with the results of Tables I and II. (b) Analogous curves resulting from an attempt to reverse the frequency order, cf. Table III and text. The corresponding control parameters, added in the inset to the phase diagram of Fig. 5(a) as solid circles, are all confined in the nonergodic phase domain.

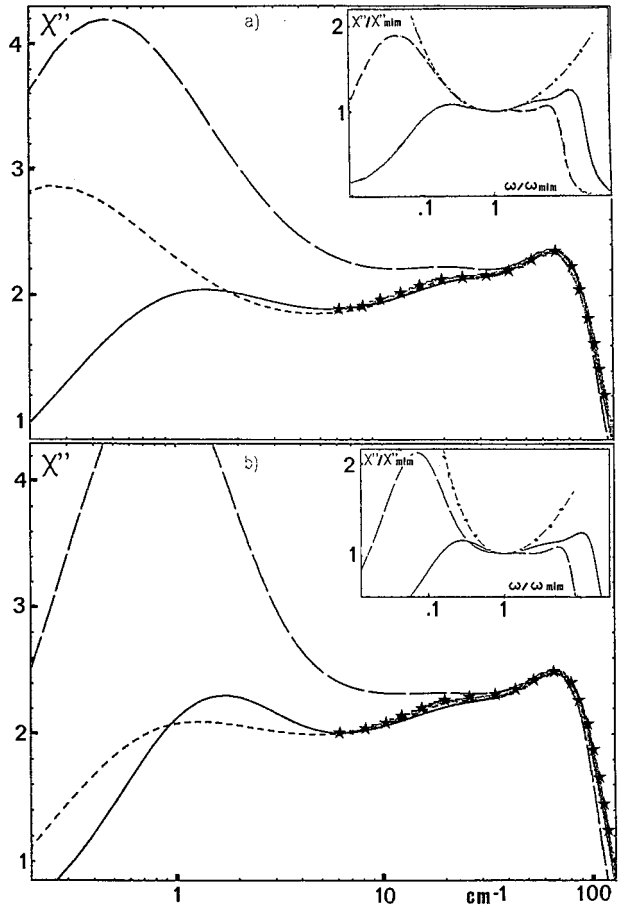

FIG. 9. Influence of squaring or not squaring the density correlators respectively as in Eqs. (3.5) or (6.1). ($\star$) Experimental data at $T=264.3$ K: The solid curves have been fitted using Eq. (3.5) as in the rest of this paper; the dashed curves are calculated through Eq. (6.1) keeping the values of the parameters as they result from the fit with Eq. (3.5) (cf. Tables I and II). The dotted curves are given by fits using Eq. (6.1). The qualities of the fits do not substantially differ from one way to the other. The α peaks, out of the fit range, are modified as well as the exponent parameter λ. (a) The F13 model, $\lambda=0.725$ and (b) the F12-model, $\lambda=0.755$. In the inset, the susceptibilities have been canonically rescaled, and the MCT master equations (Ref. 2) $\chi''(\omega) = \chi''_{\min}[b(\omega/\omega_{\min})^a + a(\omega_{\min}/\omega)^b]/(a+b)$ are plotted as dotted-dashed curves for the corresponding λ parameter.

to be restored and supports the opinion that the MCT formalism is well adapted for the description of local intermolecular relaxations processes from the THz to the GHz domain and for a large T range. For the description of the dynamical susceptibility at lower frequencies related to the structural relaxation, and temperatures below T_c, the contribution of smaller wave vectors could be more appropriate for these liquids.

Another test of the adequacy of the theory consists *a contrario* to compare the experimental data to the susceptibility of a pair of coupled oscillators with their respective frequency and damping coefficient allowed to be temperature dependent. In spite of the increased total number of parameters with a lost of physical significance, the result of the fit is made worse than those resulting from the MCT approach even, e.g., at $T\approx 214.9$ K for which the α peak is well below our frequency range.

TABLE III. Results of the free fitted frequencies.

Models	Ω_{q0} (cm^{-1})	Ω_{q1} (cm^{-1})	γ	r	D (%)
F12	23.3	25.3	1.834	2.12	1.7
F13	27.0	27.7	1.750	2.09	1.7
F0F01	11.1	45.3	0.529	0.191	1.5

Back to a more classical description of the low frequency Raman spectra, at $\omega<10$ cm^{-1}, the apparent excess of the density of relaxation states over vibrational contribution can be analyzed quantitatively when neutron and light scattering experiments are performed; the consequent determinations of the light-vibration coupling coefficient $C(\omega)$ and of the vibrational density of states $g(\omega)$ (Ref. 31) are always done at very low temperatures, in the amorphous glass and their correlated frequency dependence remain quite confusing. The main problem lies in the knowledge of the light scattering mechanism. One question among others is about the validity of the approximation of removing the convolution product in Eq. (3.1) as it has been used.[20] Figure 9 illustrates this point with two representative examples: the F13 [Fig 9(a)] and the F12 [Fig. 9(b)] models. At the same temperature $T=264.3$ K is compared to the preceding calculated spectrum a spectrum calculated with the parameters of Tables I and II (dashed lines) and with Eq. (1.5) replaced by

$$I^{\mathrm{RAMAN}}(\omega)=B'^{*}\ \mathrm{Im}\{FT[\phi_{q_0}(t)+\gamma^{*}\phi_{q_1}(t)]\}. \quad (6.1)$$

In both cases the α-peak position is shifted towards lower frequencies; the position of the minimum in the susceptibility is different and has to be rescaled; the relative height of the α and microscopic peaks and the shapes on both sides of the minimum can be slightly different as well. The F13 model, according to the following ratio,

$$\omega_{\alpha}^{\mathrm{conv}}/\omega_{\alpha}^{\mathrm{non\text{-}conv}}\approx 2^{1/\beta}, \quad (6.2)$$

where β has been introduced in Eq. (4.4d), leads to a β value around 0.37 quite small but apparently conform to other determinations on the same family of substances.[32] A rescaling of the spectra with respect to $\omega_{\min}$ and $\chi''_{\min}$ superposes the minimum region where the master equation works (see the inset of Fig. 9). Thus, when using the F13 model for *m*-toluidine, the factorization rule predicted by MCT applies in the vicinity of the minimum, the ''vicinity'' needing to be experimentally specified and certainly will require distinct frequency cutoffs. Contrary to the preceding model, the F12 model presents clear differences and the dynamical characterization of the transition is strongly affected by squaring the density correlators in Eq. (3.6). This is in agreement with the results of fits done with Eq. (6.1) to the experimental data (dotted lines) where, for the F13 model, we have obtained a good agreement between the dynamical characterization ($\lambda=0.725$ compared to 0.713), while the fit of the F12 model provides different exponents. These calculations reveal that one must be careful in using Eq. (6.1) for light scattering experiments in a large frequency range. Specific roles of kernels in this respect could be tested experimentally by a careful comparison in the intermediate β-fast process range between inelastic neutron and depolarized light scattering experiments.[33]

VII. CONCLUDING REMARKS

MCT calculations are proposed in which the effects of relaxation processes and of the phononic excitations are combined via several memory functions without any care for the spectral overlap of the microscopic, the β_{fast}, and sometimes the α processes. In contrast to other theories of glass transition, the MCT describes and evaluates all these contributions in the susceptibility spectra of a supercooled liquid in a broad T range. Moreover, distinctive spectral characteristics can be identified depending on the selected memory function.

Two density correlators have been introduced, providing a quantitative and qualitative microscopic tool for the study of these contributions applicable to the THz range spectra of both the so-called intermediate and fragile liquids. On the other hand, it could also check the relation, developed by Sokolov:[10] ''the stronger the glass is, the higher the vibrational contribution.''

Our calculations can be extrapolated down to the high frequency part of the structural α resonance, at least for the diffusive and quasihydrodynamic temperature regime above T_c. Below T_c, the formalism seems still valid for an analysis of the relaxation processes in the THz range. The raw data do not exhibit particular changes at T_c and no divergent behavior above T_g, as would be expected from a critical mechanism. Considering the set of Figs. 3 and 5, it seems plausible that behind the susceptibility spectra critical lines can be determined from the relaxational processes near the microscopic range where hopping mechanisms do not interfere.

The calculations also supply estimates, depending on the kernel, of the exponent parameter λ and the underlying parameters a and b. We expect, in the near future, to develop the calculation over a larger spectral range in order to analyze the data supplied by several scattering techniques. The gain in information should enable us to specify characteristics of chemical compounds, at a microscopic level, by the establishment of an adequate memory function.

ACKNOWLEDGMENTS

The authors are grateful to Professors H. Cummins and R. M. Pick for introducing in the theory, and to Professor Dr W. Götze for very helpful and stimulating discussions. We thank Mrs A. Colline for her constant assistance during this work and Dr A. Gerschel for critically reading the manuscript.

[1] C. A. Angell, in *Relaxation in Complex Systems*, edited by K. L. Ngai and G. B. Wright (Washington, 1984), p. 3; C. A. Angell, J. Phys. Chem. Solids **49**, 863 (1988); C. A. Angell, *Proceedings of the First Tohwa University International Symposium, Fukuoka, Japan, 1991*, AIP Conf. Proc. No. 256, edited by K. Kawasaki, T. Kawakatsu, and M. Tokuyama (AIP, New York, 1992).

[2] W. Götze, Philos. Mag. **43**, 219 (1981); W. Götze, in *Liquids, Freezing and Glass Transition (Les Houches 1989)*, edited by J. P. Hansen, D. Levesque, and J. Zinn-Justin (North-Holland, Amsterdam, 1990), and references therein; W. Götze and L. Sjögren, Rep. Prog. Phys. **55**, 241 (1992); W. Götze, Nato Advanced Study Institute, Series B, edited by T. Riste, (Kluwer Academic, New York, 1993).

[3] M. Goldstein, J. Chem. Phys. **51**, 3728 (1969).

[4] E. Rössler, J. Non-Cryst. Solids **131**, 242 (1991); Phys. Rev. Lett. **69**, 1620 (1992); in *Dynamics of Disordered Materials II*, ILL and KFA workshop Grenoble, March 1993, edited by J. Dianoux (unpublished).

[5] C. Alba, L. Busse, and C. A. Angell, J. Chem. Phys. **92**, 617 (1990).

[6] C. Alba-Simionesco and J. Fan, C. A. Angell (unpublished).

[7] J. L. Barrat, J. N. Roux, and J. P. Hansen, Chem. Phys. **149**, 197 (1990); J. N. Roux, J. L. Barrat, and J. P. Hansen, J. Phys. Condens. Matt. **1**, 7171 (1989).

[8] N. J. Tao, G. Li, and H. Z. Cummins, Phys. Rev. B **43**, 5815 (1991); Phys. Rev. Lett. **66**, 1334 (1991).

[9] (a) G. Li, W. M. Du, A. Sakai, and H. Z. Cummins, Phys. Rev. A **46**, 3343 (1992); (b) A. Patkowski, private communication; W. Steffen, A. Patkowski, H. Glaser, G. Meier, and E. W. Fisher, Phys. Rev. E (to be published).

[10] V. Malinovski, A. P. Sokolov, Solid. State Commun. **57**, 757 (1986); A. P. Sokolov, in Dynamics of Disordered Materials II, ILL and KFA workshop Grenoble, March 1993, edited by J. Dianoux (unpublished); in *Relaxation in Complex Systems*, edited by K. L. Ngai (Alicante, 1993, in press); N. J. Tao, G. Li, X. Chen, and H. Z. Cummins, Phys. Rev. A **44**, 6665 (1991); U. Buchenau, Europhys. News **24**, 77 (1993).

[11] V. Legrand, C. Alba-Simionesco, O. Delcour, and M. Descamps (unpublished); C. Alba-Simionesco, D. Morineau, and M. C. Bellissent-Funel (unpublished).

[12] G. P. Johari and M. Goldstein, J. Chem. Phys. **53**, 2372 (1970).

[13] F. Mezei, W. Knaak, and B. Farago, Phys. Rev. Lett. **58**, 571 (1987); W. Knaak, F. Mezei, and B. Farago, Europhys. Lett. **7**, 529 (1988); F. Mezei, in *Slow Dynamics in Condensed Matter, Proceedings of the First Tohwa University International Symposium, Fukuoka, Japan, 1991*, AIP Conf. Proc. No. 256, edited by K. Kawasaki, T. Kawakatsu, and M. Tokuyama; (AIP, New York 1992).

[14] (a) W. Petry, E. Bartsch, F. Fujara, M. Kiebel, H. Silescu, and B. Farago, Z. Phys. B **83**, 175 (1991); (b) M. Kiebel, E. Bartsch, O. Debus, F. Fujara,

W. Petry, and H. Silescu, Phys. Rev. B **45**, 10 301 (1992).
[15] B. Frick, D. Richter, W. Petry, and U. Buchenau, Z. Phys. B **70**, 73 (1988).
[16] J. Wüttke, M. Kiebel, E. Bartsch, F. Fujara, W. Petry, and H. Silescu, Z. Phys. B **91**, 357 (1993); J. Wüttke *et al.*, Poster at the IInd Liquid Matter Conference, Firenze, Sept. 1993.
[17] C. Alba-Simionesco and M. Krauzman (unpublished).
[18] W. Götze and L. Sjögren, J. Phys. C **21**, 3407 (1988); M. Fuchs, W. Götze, S. Hildebrand, and A. Latz, J. Phys. Condens. Matt. **4**, 7709 (1992).
[19] M. J. Stephen, Phys. Rev. **187**, 279 (1969).
[20] N. J. Tao, G. Li, X. Chen, W. M. Du, and H. Z. Cummins, Phys. Rev. A **44**, 6665 (1991).
[21] P. A. Madden, Mol. Phys. **36**, 365 (1978); P. A. Madden and T. I. Cox, *ibid*. **43**, 287 (1981); P. A. Madden and K. F. O'Sullivan, J. Chem. Phys. **90**, 1980 (1991).
[22] D. Kivelson and G. Tarjus, Phys. Rev. E **47**, (1993); D. Kivelson, W. Steffen, G. Meier, and A. Patkowski, J. Chem. Phys. **95**, 1943 (1991); A. D. Bykhowskii and R. M. Pick, *ibid*. (to be published).
[23] M. Fuchs and A. Latz, J. Chem. Phys. **95**, 7074 (1991).
[24] S. Watson and P. A. Madden, J. Chem. Phys. **99**, 6449 (1993).
[25] W. Götze, Z. Phys. B **56**, 139 (1984); W. Götze and R. Hausmann, *ibid*. **72**, 403 (1988).
[26] H. Z. Cummins, W. M. Du, M. Fuchs, W. Götze, S. Hildebrand, A. Latz, G. Li, and N. J. Tao, Phys. Rev. E **47**, 4223 (1993).
[27] (a) L. Sjögren, Phys. Rev. A **33**, 1254 (1986); G. Buchalla, U. Dersch, W. Götze, and L. Sjögren, J. Phys. C **21**, 4239 (1988); (b) J. Bosse and U. Krieger, *ibid*. **10**, 609 (1986); U. Krieger, J. Bosse, Phys. Rev. Lett. **59**, 1601 (1987).
[28] W. Götze, private communication.
[29] Note: The simplest F2 model initially developed by Bengtzelius, with two correlators $[M_{q0}(t)=v_2\phi_{q0}^2(t)$ and $M_{q1}(t)=rv_2\phi_{q0}^2(t)]$ may suggest the line shapes of the spectra; the F2 model leads to $\Omega_{q0}=37.2$ cm^{-1}; $\Gamma_{q0}=.89$; $\Omega_{q1}=21.4$ cm^{-1}; $\Gamma_{q1}=7.16$; $\gamma=2.24$; $r=3.26$; $v_{2c}=4$; $\lambda=.5$; $T_c=200.4$ K.
[30] E. Bartsch, H. Bertagnolli, G. Schulz, and P. Chieux, Ber. Bunsenges. Phys. Chem. **89**, 147 (1985); E. Bartsch, H. Bertagnolli, P. Chieux, A. David, and H. Silescu, Chem. Phys. **169**, 373 (1993).
[31] E. Duval, N. Garcia, A. Boukenter, and J. Serughetti, J. Chem. Phys. **99**, 2040 (1993); T. Achibat, A. Boukenter, and E. Duval, J. Chem. Phys. **99**, 2046 (1993).
[32] M. Cutroni, P. Migliardo, A. Piccolo, and C. Alba-Simionesco, EPS II Liquid Matter Conference, Florence, Italy 1993 (unpublished).
[33] W. Götze and L. Sjögren, J. Phys. C **21**, 3407 (1988).